CLIMATOLOGY

Vulnerability to high temperature shapes global warming impacts on rice yield

Yiwei Jian[1,2], Xuhui Wang[1]*, Jonas Jägermeyr[3,4,5], Philippe Ciais[6], Christoph Müller[5], Jakob Zscheischler[2,7], Tao Li[8], Kun Cheng[9], Pengfu Hou[10], Jianliang Huang[11], Shan Huang[12], Yu Jiang[13], Bin Wang[14], Zhenwei Song[15], Zuolin Zhang[16], Peng Zhu[17], Feng Zhou[1,18]*

Complex and spatially varying warming impacts on rice yield hinder climate change impact assessments on food security. To address this issue, we compiled a global dataset of field-warming experiments (*n* = 214) and analyzed stage-specific crop responses to temperature variations. Results show that exposures to high (30° to 35°C) and extreme high (>35°C) temperatures are the dominant drivers of warming-induced rice yield losses, primarily through harvest index reductions. One additional exposure day above 30°C during the reproductive stage reduces rice yields by 1.1 to 1.8%. In contrast, current global gridded crop models underestimate this sensitivity, simulating only 0.1 to 1.3% yield loss per exposure day. After adjusting the model biases, we estimate that global rice yield losses decrease by 8.1% under 1°C of global warming, approximately twice the unadjusted estimates, with South and Southeast Asia being the most vulnerable regions. Our results highlight the critical role of high-temperature exposure in shaping warming impacts on rice yield.

INTRODUCTION

The threat of warming-induced yield loss of rice, the staple food crop for more than half of the global population, has been acknowledged because of increasing qualitatively converging evidences (*1*–*4*). The vulnerability of global rice yield to warming, however, varies widely from −2.3 to −8.3% per 1°C of warming across studies using different approaches (*5*–*7*). The spatial variations in warming-induced yield loss are even larger (*6*–*9*), which has precluded sound scientific planning for adaptation and mitigation efforts.

Current warming impact assessments at regional or global scales often conflate the effects of increasing seasonal mean temperature with those of high-temperature exposures, thereby overlooking the fact that these two aspects of warming affect yield through distinct physiological pathways (*10*, *11*). Warmer seasonal mean temperatures not only accelerate crop development, thereby shortening the growing period and leading to less biomass accumulation (*12*), but also increase growth respiration, leading to reduced net carbon assimilation and lower assimilate availability for grain filling (*13*–*15*), particularly when nighttime warming occurs. In contrast to these gradual effects of seasonal warming, more high-temperature exposures impose stress during critical reproductive stages, such as flowering and grain filling (*16*). These events cause acute damages to enzymes, tissues, or reproductive organs and impair biomass allocation, resulting in yield losses (*17*, *18*). Without a clear distinction between the effects of increasing seasonal mean temperature and high-temperature exposures, projections of future warming impacts on crop yields may be strongly biased. For example, global crop models underestimate high temperature–induced yield losses by up to 70% in major rice-growing regions (*19*), leading to questions on the reliability of their projections (*20*–*22*).

Field-warming experiments, which expose rice to artificially elevated temperatures, are regarded as a local benchmark for yield responses to warming, although their spatial coverage is limited globally (*6*). The warming level commonly imposed (e.g., 1° or 2°C) in the experiments does not only increase seasonal mean temperature but also the exposure days of rice to high temperature (*23*). However, previous studies have not separated their distinctive effects, thereby obscuring the relative contributions of the two pathways to the observed warming impacts and the large variability among warming magnitudes and sites.

To address this research gap, we first compiled a global dataset of control and warming paired observations from the peer-reviewed literature. We then conducted warming experiments at 12 field sites in China, which increased the number of cases with high-temperature exposures of rice by 40% (see Materials and Methods). Using the combined dataset of 214 paired observations (Fig. 1A, table S1, and data S1), we quantified the yield sensitivities to high temperature during the vegetative and reproductive stages. Then, we evaluated global gridded crop models in diagnosing warming impacts on rice yield. Insights from this evaluation allows us to identify model

[1]Institute of Carbon Neutrality, Sino-French Institute for Earth System Sciences, College of Urban and Environmental Sciences, Peking University, Beijing, China. [2]Department of Compound Environmental Risks, Helmholtz Centre for Environmental Research–UFZ, Leipzig, Germany. [3]Columbia Climate School, Columbia University, New York, NY, USA. [4]NASA Goddard Institute for Space Studies (GISS), New York, NY, USA. [5]Potsdam Institute for Climate Impact Research (PIK), Member of the Leibniz Association, Potsdam, Germany. [6]Laboratoire des Sciences du Climat et de l'Environnement, LSCE/IPSL, CEA-CNRS-UVSQ, Université Paris Saclay, Gif-sur-Yvette, France. [7]Department of Hydro Sciences, TUD Dresden University of Technology, Dresden, Germany. [8]International Rice Research Institute, Los Baños, Philippines. [9]College of Resources and Environmental Sciences, Nanjing Agricultural University, Nanjing, China. [10]Jiangsu Academy of Agricultural Sciences, Nanjing, China. [11]Laboratory of Crop Ecophysiology and Farming System in the Middle Reaches of the Yangtze River, College of Plant Science and Technology, Huazhong Agricultural University, Wuhan, China. [12]Ministry of Education Key Laboratory of Crop Physiology, Ecology and Genetic Breeding, Jiangxi Agricultural University, Nanchang, China. [13]Jiangsu Collaborative Innovation Center for Modern Crop Production/Key Laboratory of Crop Physiology and Ecology in Southern China, College of Agriculture, Nanjing Agricultural University, Nanjing, China. [14]Institute of Environment and Sustainable Development in Agriculture, Chinese Academy of Agricultural Sciences/Key Laboratory of Agricultural Environment, Ministry of Agriculture and Rural Affairs, Beijing, China. [15]Institute of Crop Sciences, Chinese Academy of Agricultural Sciences/Key Laboratory of Crop Physiology and Ecology, Ministry of Agriculture and Rural Affairs, Beijing, China. [16]Hubei Key Laboratory of Food Crop Germplasm and Genetic Improvement, Institute of Food Crops, Hubei Academy of Agricultural Sciences, Wuhan, China. [17]Department of Geography, The University of Hong Kong, Hong Kong, China. [18]State Key Laboratory of Water Disaster Prevention, Jiangsu Key Laboratory of Soil and Water Processes in Watershed, College of Geography and Remote Sensing, Hohai University, Nanjing, China.
*Corresponding author. Email: xuhui.wang@pku.edu.cn (X.W.); zhouf@pku.edu.cn (F.Z.)

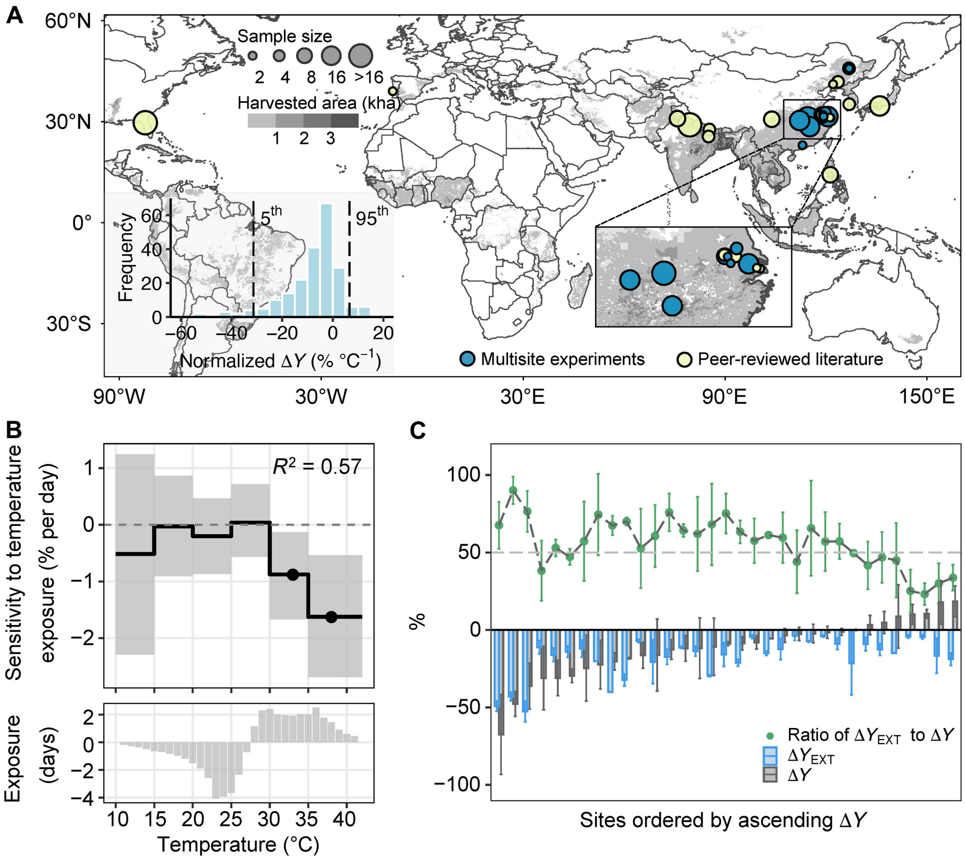

Fig. 1. High-temperature impacts on rice yield derived from global field-warming experiments. (**A**) Spatial distribution of field-warming experimental sites. Blue and green circles denote sites where we conducted warming experiments and from peer-reviewed literature, respectively, with circle areas scaled to sample size per site. The histogram illustrates the distribution of observed ΔY normalized by the magnitude of local warming ($n = 214$). Rice harvested areas are obtained from International Food Policy Research Institute (*59*). The base map of the country boundaries is from the Global Administrative Areas dataset (https://gadm.org). (**B**) Yield sensitivity to cumulative exposure days across different temperature bins during the growing season, expressed as the yield change if rice is exposed to a specific temperature bin for one additional day (*53*). Sensitivities were estimated via bootstrapping ($n = 1000$) and shown as medians. Gray-shaded areas represent 95% confidence interval (CIs) derived from 1000 sets of regression coefficients, and dots indicate coefficients significantly different from zero ($P < 0.05$, two-sided t test). R^2 represents the variance explained by both fixed (temperature exposures) and random (site-specific variations) effects. The bottom histogram displays the average difference in exposure days between control and warming treatments in each 1°C bin across all sites. (**C**) Site-level average yield changes due to increased seasonal mean temperature (ΔY; gray bar) and high temperature above 30°C (ΔY_{EXT}; blue bar), together with the ratio of ΔY_{EXT} to ΔY, ordered by ascending ΔY; error bars represent 1 SD.

biases and to develop an improved estimate of global rice yield responses to 1° and 2°C warming constrained by empirical evidence from the field-warming experiments.

RESULTS

The role of high temperature on rice yield losses

The warming impacts on rice yield (ΔY, defined as relative yield change between control and warming treatment) exhibited a large variation across experimental sites, ranging from −31.3 to 6.6% °C^{-1} (5th to 95th percentiles) when normalized by magnitude of elevated temperature (Fig. 1A). Variation in ΔY was primarily driven by differences in high-temperature exposures (i.e., cumulative exposure days when hourly temperature exceeded 30°C during the rice-growing season), which differed among sites due to variations in background temperature and the magnitude of elevated temperature (fig. S1). We then used a linear mixed-effects model to isolate high-temperature effects on rice yield, which relates ΔY to the difference in cumulative exposure days within each 5°C temperature bin between the control and warming treatments (see Materials and Methods). The results showed that exposure to high temperatures (>30°C) was significantly associated with yield reductions, with each additional day of exposure reducing yields by 0.9 to 1.6% ($P < 0.05$), while exposure to temperatures below 30°C has limited impacts on rice yield ($P > 0.1$; Fig. 1B). The adverse effect of high-temperature exposures on yield was robust across alternative model specifications, including those with different forms of temperature variables and varying definitions of temperature bin widths (3°, 4°, 6°, or 7°C; table S2).

Analyzing the yield responses to high-temperature exposure (ΔY_{EXT}) from the above model (see Materials and Methods), we found that over ~70% of experimental sites, ΔY_{EXT} is more than 50% of ΔY, indicating the wide dominance of high-temperature exposure in shaping warming impacts on rice yield. We also found that the magnitude of ΔY_{EXT} spatially correlated with ΔY ($P <$ 0.001; Fig. 1C), further confirming the critical role of high-temperature exposure.

High-temperature impacts are stage dependent

We further analyzed high-temperature impacts on rice yield formation processes including the aboveground biomass (AGB) representing biomass accumulation and harvest index (HI) representing the proportion of biomass allocated to grains. AGB and HI sensitivities to high-temperature exposures were calculated separately for the vegetative stage (when tillers are formed) and reproductive stage (when panicles and grains develop). The results revealed that warming-induced yield changes were mainly driven by reductions in HI rather than by reductions in AGB (Fig. 2A and fig. S2). High-temperature impacts on AGB and HI depend on growth stages: High temperature during the reproductive stage mainly reduced HI, whereas during the vegetative stage, it mainly reduced AGB. Specifically, HI exhibited strong sensitivity to high temperatures (>30°C) during the reproductive stage, leading to yield reductions of 1.1 to 1.8% per day of exposure. In contrast, extreme high temperatures (>35°C) during the vegetative stage mainly reduced AGB by 1.4% per day of exposure and caused yield losses of 1.5% per day of exposure, which were smaller than those observed during the reproductive stage (Fig. 2, B and C).

To gain a mechanistic understanding of stage-dependent high-temperature impacts, we analyzed data from the warming experiments at 12 field sites across China's major rice-growing regions that provide stage-specific measurements of crop phenology, morphology, and physiology (data S1). By linking high-temperature exposures to physiological and morphological traits, we identified distinct pathways through which high-temperature exposures impaired rice yield formation. During the vegetative stage, extreme-high-temperature exposures were significantly negatively correlated with net photosynthesis rate, chlorophyll content, and leaf area index ($P < 0.05$), constraining assimilate production and thereby reducing AGB (*24*). During the reproductive stage, prolonged and intense high-temperature exposures resulted in a significant decline in seed set rate, nitrogen transport efficiency, and carbon-to-nitrogen ratios of stems ($P < 0.001$), potentially disrupting carbon and nitrogen metabolisms and driving reductions in HI (table S3 and fig. S4).

Global crop models underestimated by half the warming impacts on rice yield

Projecting rice yield responses to warming regionally or globally requires typically relies on statistical approaches or process-based crop models, with the latter providing wall-to-wall coverage that extends the domain covered by sparse warming experiments. We confronted the simulated yield responses to high temperature from the Global Gridded Crop Model Intercomparison (GGCMI) phase 2 simulations (*25*) with the experimental observations (see Materials and Methods). Our analysis revealed that most crop models showed little yield change in response to high-temperature exposures (Fig. 3). Only three models (LPJmL, PEPIC, and PROMET) simulated notable rice yield loss due to high-temperature exposures. Still, the magnitude of their simulated yield loss (0.1 to 0.4% per day of exposure) is significantly lower ($P = 0.01$) than the observation {0.9% [95% confidence interval (CI): 0.1 to 1.7%] per day of exposure; Fig. 3A}. Even stronger underestimations of rice yield loss by models were found for extreme-high-temperature exposure, although most models show some degree of yield loss in this case [0.3 to 1.3% per day of exposure versus 1.6% (95% CI: 0.5 to 2.7%) per day of exposure, $P = 0.04$, Fig. 3B]. Examination across the full temperature distribution further showed that model-observation discrepancies stem from temperature above 30°C, whereas sensitivities in moderate-temperature ranges remain statistically indistinguishable (fig. S5).

This underestimation of the high-temperature impact on yield by crop models largely arose from the underrepresentation of HI responses to high temperature (Fig. 3). Most models failed to explicitly account for reproductive reduction via impaired flowering and oxidative stress, as well as possible spatial heterogeneity in sensitivities to high temperature (*26*, *27*), despite partially capturing AGB losses via reduced photosynthesis, shortened growing seasons, and consequently less biomass accumulation (figs. S6 and S7). These discrepancies underscore the need for current crop models to better incorporate high-temperature impacts to enhance the reliability of crop yield projections under future warming.

Accordingly, we performed bias correction on the global gridded crop models based on the identified model-experiment differences

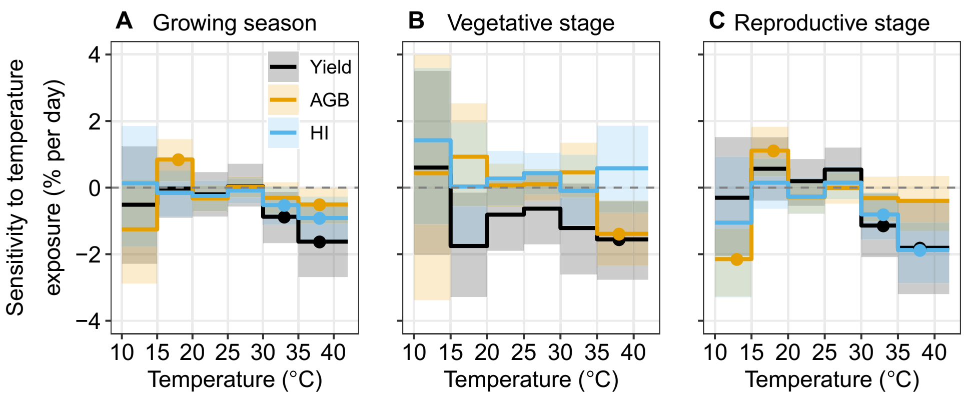

Fig. 2. Sensitivities of rice yield, AGB, and HI to high-temperature exposures. Sensitivities (i.e., regression coefficients estimated from Eq. 1 in Materials and Methods) represent the marginal responses of yield, AGB, and HI to one additional day of exposure within specific temperature bins during the entire growing season (**A**), vegetative stage (**B**), and reproductive stage (**C**). All temperature bins are explicitly included in the model specification; coefficients therefore represent the estimated effect of exposure within each bin conditional on total exposure time across bins. The stage-dependent responses remained robust using different temperature bin widths (fig. S3) and were qualitatively consistent with previous findings in other crops (*11*, *26*). Coefficients are estimated via bootstrapping ($n = 1000$) and shown as medians. Shaded areas denote 95% confidence interval derived from 1000 sets of regression coefficients, and dots indicate coefficients significantly different from zero ($P < 0.05$, two-sided t test).

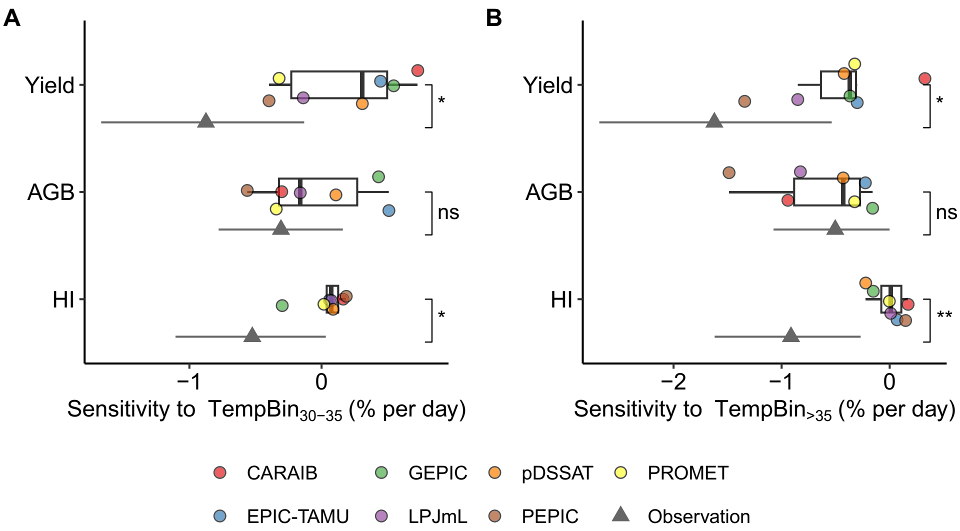

Fig. 3. Model performance in reproducing the high-temperature impacts on rice yield, AGB, and HI. (**A**) Sensitivity to high-temperature exposure (30° to 35°C). (**B**) Sensitivity to extreme-high-temperature exposure (>35°C). Sensitivities are defined in the same way as in Fig. 2. For yield and its components (AGB and HI), box-and-whisker plots show the distribution of sensitivities across seven crop models (colored dots), with the median marked. Edges are the first and third quartiles, and whiskers extend to 1.5 times the interquartile range. The triangles indicate the sensitivities derived from field-warming experiment observations, with error bars showing the 95% CIs. Statistical significance of differences between observed and simulated sensitivities was assessed using a two-sided *z*-score test (ns, $P \geq 0.05$; *$P < 0.05$; **$P < 0.01$).

in sensitivity to high-temperature exposure (see Materials and Methods), to provide an observation-constrained global estimate of the rice yield response to warming. This approach maps the observed high-temperature effects from experimental sites to the global scale, which aligns well with the observations (Wilcoxon rank sum test, $P > 0.05$; fig. S8).

By jointly using the bias-corrected and spatially explicit sensitivity estimates and pattern of projected warming by Coupled Model Intercomparison Project phase 6 (CMIP6) Earth system models (see Materials and Methods), we projected that, under 1°C increase in global mean temperature, global rice yield reductions (weighted by harvested area) amount to 8.1 ± 2.3% (ensemble means ± 1 SD), which is double that of the original model ensemble (3.8 ± 1.7%, $P < 0.01$). There were pronounced spatial variations in the magnitude of correction, indicated by the differences between the original simulation ($\Delta Y^{\text{original}}$; Fig. 4A) and the bias-corrected yield projection ($\Delta Y^{\text{bias-corrected}}$; Fig. 4B). In South and Southeast Asia, yield losses were substantially underestimated in the original simulations, increased from 2.1 to 6.6% in Pakistan, India, and Bangladesh after bias correction and from 3.7% to 7.7% in Thailand, the Philippines, and Myanmar, largely due to large dose of high-temperature exposures (Fig. 4C and figs. S9 and S10). In contrast, East Asian countries such as China and Japan exhibited smaller underestimations (<2%). A similar pattern emerged under the 2°C of global warming but with larger yield reductions (fig. S11).

DISCUSSION

Methodologically, our study improves the rice yield response to high-temperature exposure in current models by proposing a postsimulation adjustment to global crop model simulations, resulting in a 8.1% global rice yield loss in response to 1°C of global warming compared to 3.8% before adjustment. The magnitude and spatial pattern of warming impacts are mainly shaped by the effects of high-temperature exposure that increase with global warming. Our observation-constrained estimate is consistent with field warming experiments but is double that of the original model ensemble and close to the upper bound of previous estimates (*5*–*7*). Compared with earlier emergent-constraint studies that relied on aggregated temperature sensitivity (*5*, *6*), our approach explicitly separates nonlinear heat stress effects from changes in seasonal mean temperature. This distinction is critical because warming simultaneously shifts mean climate and increases exposure to extreme heat, which affects rice yield through distinct physiological pathways. In contrast to global statistical models that infer responses from historical correlations and implicitly embed adaptation (*7*, *8*, *28*), our results reveal more severe damage from extreme heat than previously recognized, which is also in line with recent statistical analyses on global crop yield finding temperature anomalies in the high end causing larger yield loss (*29*).

Because the warming impacts are largely shaped by the high-temperature effects, the uncertainty in the assessment thus lies mostly in estimating the exposure and vulnerability of rice yields to high temperatures. A temperature of 30°C is a widely used threshold to detect the heat exposure for many crops, which is also consistent with our analyses. Recent studies indicate that the threshold could also vary from region to region due to adaptive managements (*30*). Although the dose of heat exposure could vary, our sensitivity analyses using various thresholds show qualitatively similar results (figs. S3 and S6).

Our results also suggest that the stress of high-temperature exposure on rice yield is less in biomass but more in processes controlling the HI, such as carbon allocation, grain formation, and grain filling. High temperatures around anthesis cause spikelet sterility by disrupting pollen viability and fertilization, resulting in a reduced seed set rate and substantial yield loss (*31*). Beyond reproductive failures, high temperatures accelerate grain filling while suppressing starch synthesis by down-regulating key starch-accumulation enzymes, inhibiting nitrogen transfer from stems to grains, and ultimately

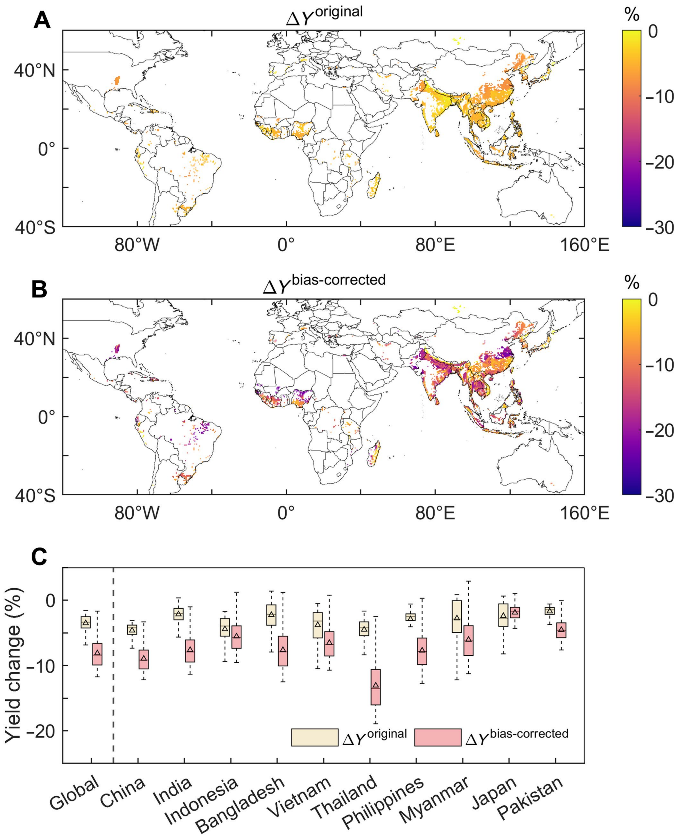

Fig. 4. Rice yield changes under 1°C of global warming before and after bias corrections. (**A**) Spatial pattern of rice yield changes ($\Delta Y^{original}$, %) under 1°C of global warming based on GGCMI phase 2 simulations, scaled using local warming magnitude from five CMIP6 models. Data are shown as multimodel ensemble means from seven global gridded crop models and five global climate models in the SSP5-8.5 scenario. (**B**) Spatial pattern of bias-corrected yield ($\Delta Y^{bias\text{-}corrected}$, %) under 1°C of global warming. Data are shown as the ensemble mean of 35,000 realizations incorporating uncertainties from crop models ($n = 7$), climate models ($n = 5$), and empirically derived yield sensitivities to high temperature (>30°C) via Monte Carlo simulations ($n = 1000$). (**C**) Distribution of national-level yield changes among the top 10 rice producing countries, ranked by total production (*41*). Box-and-whisker plots show the spread of area-weighted national means for $\Delta Y^{original}$ and $\Delta Y^{bias\text{-}corrected}$ across 35,000 ensemble members. Medians are marked as horizontal lines, and box edges are the first and third quartile. Whiskers extend to 1.5 × interquartile range, and triangles represent the ensemble means. There were significant differences between $\Delta Y^{original}$ and $\Delta Y^{bias\text{-}corrected}$ ($P < 0.001$) both at the global and national levels based on the Wilcoxon rank sum test. Rice harvested areas are obtained from International Food Policy Research Institute (*59*). The base map of the country boundaries is from the Global Administrative Areas dataset (https://gadm.org).

reducing grain weight and HI (*32*, *33*). In addition, assimilate transport to grains is constrained by phloem blockage or down-regulated sucrose transporters, further limiting carbohydrate supply and source-sink balance (*34*, *35*). Hormonal imbalances (reduced auxin and cytokinin levels) also impair panicle development and sink strength (*36*).

Our estimates should be interpreted within the context of physiological effects. The temperature-yield relationships are derived from single-factor warming experiments, which allow us to isolate high-temperature effects from confounding water and nutrient stresses. However, these experimental conditions may differ from farmer-managed fields, where yield outcomes also depend on complex interactions among temperature, water availability, crop physiology, and canopy energy balance (*37*). In particular, crop heat stress is mediated by canopy temperature rather than near-surface air temperature. Because our global estimates rely on large-scale air temperatures, they do not fully reflect irrigation-induced evaporative cooling, which can substantially reduce canopy temperature relative to the surrounding air (*38*–*40*). Consequently, our estimates for irrigated rice, which account for 75% of global rice production (*41*), represent the yield loss driven by heat stress without possible canopy cooling effects from irrigation. Conversely, in rainfed systems, yield losses associated with high temperatures are likely to be amplified by the compounding effects of thermal and hydrological stress losses via vapor pressure deficit–induced stomatal closure and inhibited biomass accumulation (*42*, *43*). Supplementary analyses using GGCMI phase 2 outputs suggest that rainfed rice systems are generally more sensitive to high temperatures, reflecting compounding heat-water stress interactions, although the magnitude of this amplification remains uncertain (fig. S18). These results highlight the critical need for future studies to explicitly address complex heat-water interactions under climate change, as compound heat and moisture extremes are projected to intensify (*44*, *45*). The systematic underestimation of high-temperature effects by global crop models that we found is consistent with previous analyses (*19*, *22*, *42*, *46*, *47*), which is expected, given that the processes mentioned above have not been taken account in these models. While it urgently calls for incorporating these processes, the bias-corrected estimates provide a remedy before the long model improvement process completes. Our estimates also highlight South and Southeast Asia as hotspots of compound heat exposure and vulnerability (Fig. 4). It therefore requests region-tailored, climate-resilient adaptations, such as adopting heat-tolerant crop cultivars (*48*, *49*), optimizing irrigation practices (*50*, *51*), and enhancing soil quality that buffers against high-temperature stress (*27*).

MATERIALS AND METHODS

Field-warming experiment dataset

To investigate high-temperature impacts on rice yield, we first compiled a global dataset of field-warming experiments from the peer-reviewed literature then conducted the warming experiments in China for supplementing the cases of high-temperature exposure of rice. Literature-based data were selected on the basis of the following criteria: (i) Experiments conducted under irrigated rice systems in open fields; (ii) warming treatments applied continuously (24 hours) or during daytime for the entire growing season or for more than 2 months covering the reproductive stage; (iii) free-air infrared heating of crop canopy or near-surface air under ambient environmental conditions; and (iv) studies reported both control and warming treatment outcomes, including warming magnitude, timing, and rice yields. This yielded a dataset comprising 128 paired observations at 17 sites. Notably, experiments with nighttime warming were excluded. While warmer nights reduce yields mainly via source limitation (e.g., increased respiration) (*13*–*15*), this study specifically targets the nonlinear, upper tail of the temperature distribution. Restricting data to daytime and all-day warming isolates the acute, threshold-dependent sink limitations (e.g., pollen sterility) that structurally drive yield loss under extreme heat (*17*). For each observation, six categories of information were collected: (i) yield-related variables such as actual yield, AGB, and HI; (ii) warming treatment characteristics such as magnitude, timing, and duration; (iii) management practices such as nitrogen application rate, dates of transplanting, booting, flowering, and maturity, and rice cultivar; (iv) climatic variables such as daily mean and maximum temperature and cumulative growing season precipitation (GSP); (v) soil properties such as clay content, organic carbon, bulk density, total nitrogen, and pH in topsoil; and (vi) experimental information such geographic location and year.

To cover a broader range of high-temperature exposures, we conducted the multisite field-warming experiments at 12 sites across major rice-growing regions in China. All sites followed standardized protocols under irrigation conditions, with continuous free-air heating applied over the entire growing season. The imposed warming levels varied from 0.5° to 4°C across experiments. In addition to the six categories of information mentioned above, our experiments recorded crop morphological and physiological traits during the vegetative and reproductive stages (e.g., leaf area index, photosynthetic rate, and carbon and nitrogen uptake in stems, leaves, and grains), enabling the mechanistic analyses on how high temperature affects yield formation processes. The experiment provided 86 paired observations, increasing the number of cases with high-temperature exposures by 40% compared to literature-based data (fig. S12). A list of 214 paired observations is provided in data S1.

We further assessed data representativeness by identifying grid cells with similar growing season temperature (GST) and GSP to the experimental sites, with a difference in GST < 1°C and GSP < 150 mm (*6*). Results indicated that the field-warming dataset can generally represent the climate characteristics of ~80% of global rice-growing area. This evaluation was extended to annual mean temperature (MAT) and annual mean precipitation (MAP), and yielded consistent results across metrics (fig. S13).

Statistical analysis of yield responses to high temperature

To quantify high-temperature stress in field-warming experiments, we first constructed hourly temperature time series for each paired control-warming experiment. Daily maximum and minimum temperatures were sourced from on-site observations when available and interpolated to hourly values using a sinusoidal interpolation (*52*, *53*). Where site-level temperature data were unavailable, we used ERA5 hourly data (the fifth generation reanalysis dataset of European Centre for Medium-Range Weather Forecasts) as a baseline temperature. For warming treatments, ERA5-based temperatures were adjusted by adding the warming magnitude (ΔT) during the treatment periods, based on reported timing and duration. Temperature exposure was then defined as the total exposure days (24 hours) of rice plants within each 1°C bin over the growing season, following Schlenker and Roberts (*53*).

We then developed a linear mixed-effects model to quantify the high-temperature impacts on rice yield while avoiding the confounding effects of seasonal mean temperature increase. The model assumes that yield change was nonlinearly related to cumulative exposure days within each temperature bin (*53*)

$$\Delta Y_{ijt} = \alpha_0 + \sum_{h=1}^{N} \delta_h \times \Delta \mathrm{TempBin}_{ijth} + \mathrm{Studysite}_i + \varepsilon_{ijt} \quad (1)$$

where ΔY_{ijt} refers to the warming impact on rice yield (%) at site i, experiment j, and year t, quantifying as relative yield change between control and warming treatment groups. $\Delta\mathrm{TempBin}_{ijth}$ represents the difference of cumulative exposure days to temperature bin h between the control and warming treatments throughout the growing season. Temperatures were aggregated into 5°C bins spanning the full temperature range of observed growing-season conditions. Exposure below 10°C occurs too infrequently during the rice-growing season in our dataset to support reliable estimation and is therefore excluded from the binned specification (fig. S14). This choice of bin width avoids overfitting caused by sparse samples at finer bin widths and maintains flexibility to capture nonlinear responses. Our main specification uses a full-bin parameterization across the retained temperature range to characterize the marginal yield sensitivity across the full temperature distribution under warming and quantify the contribution of each temperature bin to yield variation. δ_h refers to the yield sensitivity, expressed as the yield change per additional day of exposure in bin h. $\mathrm{Studysite}_i$ is the random-effect term accounting for the variability of background conditions across study sites, and ε_{ijt} is the residual error [$\varepsilon_{ijt} \sim N(0, \sigma^2)$]. The model incorporated weights that accounted for intersite differences in sampling frequency and replication, using site-level weights proportional to the number of available observations at each site. Water stress was not considered because irrigation was applied in all experiments. Other climatic or management factors were excluded because of weak correlation with ΔY (fig. S15).

To quantify yield loss due to high-temperature exposure, we first calculated the yield change associated with each temperature bin by multiplying the estimated coefficients (δ_h) with the corresponding exposure days (*42*, *54*). High temperature–induced yield loss (ΔY_{EXT}) was then defined as the cumulative impacts from temperature bins with significantly negative coefficients ($\delta_h < 0$ and $P < 0.05$)

$$\Delta Y_{\mathrm{EXT},ijt} = \sum_{h \in H} \delta_h \times \mathrm{TempBin}_{ijth} \quad (2)$$

where H denotes the corresponding set of temperature bins. In this study, these bins correspond to the high-temperature (30° to 35°C) and extreme-high-temperature (>35°C) ranges. Last, the contribution of high-temperature stress to the total warming-induced yield changes was quantified as the fraction of the absolute yield change attributable to high temperature relative to the total absolute yield change induced by warming

$$\mathrm{Ratio}_{ijt} = \frac{|\Delta Y_{\mathrm{EXT},ijt}|}{|\Delta Y_{\mathrm{EXT},ijt}| + |\Delta Y_{ijt} - \Delta Y_{\mathrm{EXT},ijt}|} \times 100\% \quad (3)$$

The stage-dependent high-temperature effects were further examined by relating rice yield and yield components (AGB and HI) to temperature exposures during the vegetative and reproductive stages, using the same approach as in Eq. 1.

Robustness checks

To assess the robustness of our estimated temperature-yield response and ensure that specific modeling choice does not drive the conclusion, we test a series of alternative model specifications.

1) M1: Model using the absolute temperature exposures in warming treatments as independent variables, which define the real thermal environment experienced by the crop

$$\Delta Y_{ijt} = \alpha_0 + \sum_{h=1}^{N} \delta_h \times \mathrm{TempBin}_{ijth} + \mathrm{Studysite}_i + \varepsilon_{ijt} \quad (4)$$

where $\mathrm{TempBin}_{ijth}$ represents the cumulative exposure days to temperature bin h under the warming treatments throughout the growing season.

2) M2: Model includes an alternative low-temperature specification. Although exposure below 10°C is negligible in our dataset, we merge observations below 10°C with those in the range of 10° to 15°C to form a unified <15°C bin. This specification is used to assess whether the estimated temperature-yield response is sensitive to the treatment of sparse low-temperature exposure.

3) M3: Model with site fixed intercepts. The site random effect is replaced with the fixed effect, which allows us to evaluate the sensitivity of temperature response to different assumptions about between-site variation.

4) M4: Model using growing degree days (GDDs) as independent variables. This piecewise linear approach regressed yield changes against growing degree days accumulated over the growing season (*53*). Three types of GDDs ($\mathrm{GDD}_{\mathrm{low}}$, $\mathrm{GDD}_{\mathrm{med}}$, and $\mathrm{GDD}_{\mathrm{high}}$) were used to characterize the nonuniform yield response to different temperature exposures. They share a similar equation but with different thresholds

$$\mathrm{GDD}_{T1}^{T2} = \sum_{h=1}^{N} \mathrm{DD}_h / 24, \mathrm{DD}_h = \begin{cases} 0 \text{ when } T_h \le T_1 \\ T_h - T_1 \text{ when } T_1 < T_h \le T_2 \\ T_2 - T_1 \text{ when } T_h - T_2 \end{cases} \quad (5)$$

where T_h represents surface air temperature at hour h and N is the total number of hours in the growing season. Hourly temperature data are obtained from site observations and ERA5 reanalysis dataset. T_1 and T_2 indicate the lower and upper temperature thresholds of GDD, respectively. Next, we built the regression model to explain experimental yield changes to warming based on degree day

$$\Delta Y_{ijt} = \alpha_0 + \delta_{\mathrm{low}} \times \Delta\mathrm{GDD}_{\mathrm{low},\ ijth} + \delta_{\mathrm{med}} \times \Delta\mathrm{GDD}_{\mathrm{med},\ ijth} + \delta_{\mathrm{high}} \times \Delta\mathrm{GDD}_{\mathrm{high},\ ijth} + \mathrm{Studysite}_i + \varepsilon_{ijt} \quad (6)$$

where $\Delta\mathrm{GDD}_{\mathrm{low}}$, $\Delta\mathrm{GDD}_{\mathrm{med}}$, and $\Delta\mathrm{GDD}_{\mathrm{high}}$ represent the difference of degree days between control and warming treatments, respectively. δ refers to the yield sensitivity, expressed as the yield change per additional degree day of exposure. All possible degree day thresholds were tested using this model, and the final thresholds were determined by the model that maximized the explanatory power (highest R^2). Specifically, we use $\mathrm{GDD}_{-\infty}^{15}$, GDD_{15}^{33}, and $\mathrm{GDD}_{33}^{\infty}$ to characterize growing season $\mathrm{GDD}_{\mathrm{low}}$, $\mathrm{GDD}_{\mathrm{med}}$, and $\mathrm{GDD}_{\mathrm{high}}$.

5) M5, M6, M7, and M8: Model using different temperature bin widths (3°, 4°, 6°, and 7°C). Using these alternative bin widths can effectively test whether the shape of the nonlinearities in our baseline estimates is driven by our preferred specifications of bins.

6) M9: Model with an omitted reference temperature bin. To assess whether the estimated temperature-yield response is sensitive to the choice of parameterization, we additionally estimate a specification in which the 25° to 30°C bin is omitted and treated as the reference category. Under this specification, all coefficients are interpreted relative to the temperature range of 25° to 30°C.

To account for the statistical uncertainty of the baseline model (Eq. 1) and these alternative models, we run each model with 1000 bootstrap. The 1000 sets of estimated regression coefficients are then used to determine the CIs of coefficients, and their medians are used to determine the response curves. We also evaluated model robustness using leave-one-out cross-validation with site-block partitioning. For each iteration, one randomly selected site served as the test data, while the model was trained on the remaining sites to calculate the root mean square error and mean square error. The performance of each model was presented in table S2.

Assessments of crop model responses to high temperature

To assess the capability of process-based crop models to replicate observed negative yield responses to high temperatures, we used simulation data from GGCMI phase 2 experiment. This dataset provides crop yield simulations at 0.5° spatial resolution from 1980 to 2010, driven by the AgMIP (Agricultural Model Intercomparison and Improvement Project) Modern-Era Retrospective Analysis for Research and Applications (AgMERRA) climate dataset (*55*), and involves systematical perturbation of climate and management factors (temperature, precipitation, CO_2 levels, and applied nitrogen level) to isolate their individual effect on crop yields (*25*). For the comparison with observations, we extracted a subset of simulations designed to isolate the temperature effect. Specifically, we selected simulations with uniform temperature increases of 1°, 2°, and 3°C during the rice-growing season across all grid cells, while maintaining constant CO_2 concentration at 360 parts per million, nitrogen application rates of 200 kg N ha^{-1}, and irrigated scenarios without water constraints. Seven models (CARAIB, EPIC-TAMU, GEPIC, LPJmL, pDSSAT, PEPIC, and PROMET) were eventually selected for the assessments (table S4).

To evaluate simulated sensitivity to high temperature, the warming effect on simulated rice yield (ΔY) was defined as the relative yield change between the baseline simulation ($T + 0$) and the warming scenarios ($T + n$, where n = 1°, 2°, or 3°C). Yield changes from each model were first detrended to remove the long-term trends (ΔY^{de}) and then regressed against temperature exposures derived from AgMERRA. Temperature exposures for each grid cell and warming scenario were calculated following the same procedure as for the observational dataset. The statistical model was specified as

$$\Delta Y_{itw}^{\mathrm{de}} = \Delta Y_{itw} - \left(\alpha_{i,w} \times \mathrm{Year}_t + \beta_{i,w}\right) + \overline{Y}_{i,w}, \forall i,\ w \quad (7)$$

$$\Delta Y_{itw}^{\mathrm{de}} = \alpha_0 + \sum\nolimits_{h=1}^{N} \delta_h \times \Delta\mathrm{TempBin}_{ithw} + \mathrm{grid}_i + \varepsilon_{itw} \quad (8)$$

where i, t, and w refer to grid cell, year, and warming scenario, respectively. $\overline{Y}_{i,w}$ represents the mean yield change during 1980–2010; grid_i is included as a random effect to account for spatial clustering.

The resulting regression coefficients from seven models were compared with those estimated from field-warming experiments. Comparability was ensured by consistent temperature exposure distributions and identical sensitivity estimation methods. Although the model simulations had a coarser spatial resolution (0.5°), the distribution of exposures remained statistically similar to that of field observations (Kolmogorov-Smirnov test, P = 0.61; fig. S16), indicating that the lower simulated sensitivities were not attributable to insufficient representation of high-temperature exposure. The same procedures were applied to simulated AGB and HI. All analyses were repeated for different temperature bins and each warming scenario (figs. S6 and S17). In addition, we analyzed the simulated temperature responses under rainfed scenarios using five crop models (CARAIB, EPIC-TAMU, LPJmL, pDSSAT, and PROMET; table S4). Simulated sensitivities to high temperatures were estimated following the same procedure as for irrigated simulations. The result indicated that rainfed rice is more sensitive to high temperatures than irrigated systems (fig. S18).

Bias corrections of simulated yield responses to warming

Most process-based crop models are limited in capturing the full effects of high temperature on the HI, as well as spatial heterogeneity in sensitivities to high-temperature exposures. To address these limitations, we performed an observation-constrained bias correction on the GGCMI phase 2 simulations, explicitly targeting the sensitivities to temperatures above 30°C where systematic model deficiencies were identified (Fig. 3 and fig. S5). This approach provides an improved observation-constrained global assessment of warming impacts on rice yield through two main steps: (i) refining sensitivity to high-temperature exposure to account for its spatial variation and (ii) applying the corrected sensitivities to adjust projected yield changes under warming at global and regional scales (fig. S19).

To better represent the spatial heterogeneity in yield responses to high temperatures and improve the accuracy of regression model, we first identified key drivers by calculating the Pearson correlations between observed ΔY and variables across three domains: (i) climate conditions (annual and growing-season temperature, precipitation, and solar radiation), (ii) soil properties (organic carbon, clay content, bulk density, total nitrogen, and pH), and (iii) management practices (application rate of nitrogen, phosphorus, and potassium; rice type: indica, japonica, and hybrid). To reduce collinearity, we performed principal components analysis (PCA) within each domain and constructed composite indices from components cumulatively explained 90% of the variance (table S5). These composite indices were then incorporated as interaction terms with high-temperature exposures in the Eq. 1, and the optimal model was selected on the basis of the significance of interaction terms, the coefficient of determination (R^2), and changes in the Akaike information criterion (ΔAIC) compared to Eq. 1.

The results revealed soil properties as the dominant driver in determining the spatial variation in yield sensitivity to high temperatures ($R^2 = 0.56$ and $\Delta\text{AIC} = -17.1$), whereas climate and management factors were not significant (Chi-square test, $P > 0.05$) within the range of variability represented by experimental conditions (table S6 and see further discussion in Supplementary Text). Using the refined model, yield sensitivity to high temperatures can be expressed as a linear function of soil, expressed as $\delta_{30-35} + \beta_{30-35}\text{Soil}$ and $\delta_{>35} + \beta_{>35}\text{Soil}$, where δ represents the average response and β captures the modulation by soil properties. Grid-specific sensitivities of crop models were derived analogously by introducing interaction terms between soil properties and high-temperature exposure into Eq. 8.

Building on the refined, spatially varying sensitivities, we next applied bias correction to simulated yield responses to account for high-temperature effects under plausible future warming. First, the original GGCMI phase 2 yield responses ($\Delta Y^{\text{original}}$) were rescaled from uniform temperature perturbations (+1°, +2°, and +3°C) to grid-specific local warming levels (ΔT) derived from five CMIP6 models (GFDL-ESM4, IPSL-CM6A-LR, MPI-ESM1-2-HR, MRI-ESM2-0, and UKESM1-0-LL) under the SSP5-8.5 scenario. For each climate model, we first identified a 30-year period during which the global mean temperature increased by 1° or 2°C relative to 1980–2010. We then calculated the corresponding grid-specific local warming (ΔT) over this period. A linear or quadratic function, whichever yielded a higher R^2 for the specific grid cell, was fitted between the $\Delta Y^{\text{original}}$ and the imposed warming magnitude (+1°, 2°, and 3°C), and this function was interpolated to grid-specific ΔT to obtain rescaled yield responses under realistic future warming. In addition, high-temperature exposures associated with grid-specific warming were derived in an analogous "delta change" manner (*56*, *57*). Grid-level exposure-warming relationships were constructed using AgMERRA dataset and interpolated to the CMIP6-derived ΔT.

Next, we extrapolated the spatially varying high-temperature sensitivities to estimate impacts of high temperatures on yields across global rice paddies. This estimation assumes that the empirical relationship between high temperatures and rice yields applies globally, without considering other potential effects. The expected high-temperature impacts are calculated as

$$\Delta Y^{\text{obs}}_{\text{EXT},itw} = \left(\delta^{\text{obs}}_{30-35} + \beta^{\text{obs}}_{30-35}\text{Soil}_i\right) \times \text{TempBin}_{itw,30-35} + \left(\delta^{\text{obs}}_{>35} + \beta^{\text{obs}}_{>35}\text{Soil}_i\right) \times \text{TempBin}_{itw,>35} \tag{9}$$

$$\Delta Y^{\text{sim}}_{\text{EXT},itw} = \left(\delta^{\text{sim}}_{30-35} + \beta^{\text{sim}}_{30-35}\text{Soil}_i\right) \times \text{TempBin}_{itw,30-35} + \left(\delta^{\text{sim}}_{>35} + \beta^{\text{sim}}_{>35}\text{Soil}_i\right) \times \text{TempBin}_{itw,>35} \tag{10}$$

where $\text{TempBin}_{itw,30-35}$ and $\text{TempBin}_{itw,>35}$ were derived from the AgMERRA dataset and were also rescaled to local warming levels. Soil_i is computed by applying PCA loadings to gridded soil properties from the Harmonized World Soil Database v 1.2 (*58*), which were also used to construct the PCA components for all experimental sites. "obs" and "sim" represent coefficients derived from experimental data and crop model output, respectively.

Last, we adjusted the rescaled $\Delta Y^{\text{original}}$ by incorporating observed high-temperature effects to obtain bias-corrected yield changes ($\Delta Y^{\text{bias-corrected}}$)

$$\Delta Y^{\text{bias-adjusted}}_{itw} = \Delta Y^{\text{original}}_{itw} - \Delta Y^{\text{sim}}_{\text{EXT},itw} + \Delta Y^{\text{obs}}_{\text{EXT},itw} \tag{11}$$

We also conducted a sensitivity analysis by further constraining crop model responses within moderate-temperature interval to match the empirically estimated response from experiments. This additional correction only slightly amplified projected warming-induced yield losses, but the overall magnitude of change remained modest (fig. S20).

Uncertainty analysis

To assess the overall uncertainty in bias-corrected yield changes, we used a Monte Carlo simulation accounting for three independent sources of uncertainty: structural uncertainty from crop models, uncertainty in climate projections, and statistical uncertainty in the empirically derived high-temperature sensitivities (β). For each grid cell, β values were randomly sampled ($n = 1000$) from the multivariate normal distribution defined by the estimated means and joint covariance matrix of regression coefficients. These were combined with yield projections from seven global gridded crop models and five global climate models, resulting in an ensemble of 35,000 realizations (i.e., $7 \times 5 \times 1000$) for each warming level (+1° and

2°C). Spatial patterns of $\Delta Y^{\text{bias-corrected}}$ were derived from the ensemble mean. Global and national yield responses were calculated as harvested area-weighted means across all rice-growing grid cells and realizations. We further decomposed the contribution of each uncertainty source using a three-way analysis of variance (ANOVA), revealing that uncertainty associated with crop models and the statistical uncertainty in the empirically derived high-temperature sensitivities dominated the total variance, whereas the contribution from climate projections is comparatively smaller (figs. S21 and S22).

Supplementary Materials

The PDF file includes:

Supplementary Text
Figs. S1 to S22
Tables S1 to S6
Legend for data S1
References

Other Supplementary Material for this manuscript includes the following:

Data S1

REFERENCES

1. D. B. Lobell, S. Di Tommaso, A half- century of climate change in major agricultural regions: Trends, impacts, and surprises. *Proc. Natl. Acad. Sci. U.S.A.* **122**, e2502789122 (2025).
2. E. E. Rezaei, H. Webber, S. Asseng, K. Boote, J. L. Durand, F. Ewert, P. Martre, D. S. MacCarthy, Climate change impacts on crop yields. *Nat. Rev. Earth. Environ.* **4**, 831–846 (2023).
3. R. Bezner Kerr, T. Hasegawa, R. Lasco, I. Bhatt, D. Deryng, A. Farrell, H. Gurney-Smith, H. Ju, S. Lluch-Cota, F. Meza, G. Nelson, H. Neufeldt, P. Thornton, "Food, fibre, and other ecosystem products," in *Climate Change 2022: Impacts, Adaptation and Vulnerability*, H.-O. Pörtner, D. C. Roberts, M. Tignor, E. S. Poloczanska, K. Mintenbeck, A. Alegría, M. Craig, S. Langsdorf, S. Löschke, V. Möller, A. Okem, B. Rama, Eds. (Cambridge Univ. Press, 2022), pp. 713–906.
4. A. J. Challinor, J. Watson, D. B. Lobell, S. M. Howden, D. R. Smith, N. Chhetri, A meta-analysis of crop yield under climate change and adaptation. *Nat. Clim. Chang.* **4**, 287–291 (2014).
5. C. Zhao, S. Piao, X. Wang, Y. Huang, P. Ciais, J. Elliott, M. Huang, I. A. Janssens, T. Li, X. Lian, Y. Liu, C. Müller, S. Peng, T. Wang, Z. Zeng, J. Peñuelas, Plausible rice yield losses under future climate warming. *Nat. Plants* **3**, 16202 (2017).
6. X. Wang, C. Zhao, C. Müller, C. Wang, P. Ciais, I. Janssens, J. Peñuelas, S. Asseng, T. Li, J. Elliott, Y. Huang, L. Li, S. Piao, Emergent constraint on crop yield response to warmer temperature from field experiments. *Nat. Sustain.* **3**, 908–916 (2020).
7. T. Hasegawa, H. Wakatsuki, H. Ju, S. Vyas, G. C. Nelson, A. Farrell, D. Deryng, F. Meza, D. Makowski, A global dataset for the projected impacts of climate change on four major crops. *Sci. Data* **9**, 58 (2022).
8. P. Agnolucci, C. Rapti, P. Alexander, V. De Lipsis, R. A. Holland, F. Eigenbrod, P. Ekins, Impacts of rising temperatures and farm management practices on global yields of 18 crops. *Nat. Food* **1**, 562–571 (2020).
9. J. Jägermeyr, C. Müller, A. C. Ruane, J. Elliott, J. Balkovic, O. Castillo, B. Faye, I. Foster, C. Folberth, J. A. Franke, K. Fuchs, J. R. Guarin, J. Heinke, G. Hoogenboom, T. Iizumi, A. K. Jain, D. Kelly, N. Khabarov, S. Lange, T.-S. Lin, W. Liu, O. Mialyk, S. Minoli, E. J. Moyer, M. Okada, M. Phillips, C. Porter, S. S. Rabin, C. Scheer, J. M. Schneider, J. F. Schyns, R. Skalsky, A. Smerald, T. Stella, H. Stephens, H. Webber, F. Zabel, C. Rosenzweig, Climate impacts on global agriculture emerge earlier in new generation of climate and crop models. *Nat. Food* **2**, 873–885 (2021).
10. J. Tack, A. Barkley, L. L. Nalley, Effect of warming temperatures on US wheat yields. *Proc. Natl. Acad. Sci. U.S.A.* **112**, 6931–6936 (2015).
11. M. B. Espe, J. E. Hill, R. J. Hijmans, K. McKenzie, R. Mutters, L. A. Espino, M. Leinfelder-Miles, C. van Kessel, B. A. Linquist, Point stresses during reproductive stage rather than warming seasonal temperature determine yield in temperate rice. *Glob. Chang. Biol.* **23**, 4386–4395 (2017).
12. Z. Fatima, M. Ahmed, M. Hussain, G. Abbas, S. Ul-Allah, S. Ahmad, N. Ahmed, M. A. Ali, G. Sarwar, E. U. Haque, P. Iqbal, S. Hussain, The fingerprints of climate warming on cereal crops phenology and adaptation options. *Sci. Rep.* **10**, 18013 (2020).
13. S. Peng, J. Huang, J. E. Sheehy, R. C. Laza, R. M. Visperas, X. Zhong, G. S. Centeno, G. S. Khush, K. G. Cassman, Rice yields decline with higher night temperature from global warming. *Proc. Natl. Acad. Sci. U.S.A.* **101**, 9971–9975 (2004).
14. J. R. Welch, J. R. Vincent, M. Auffhammer, P. F. Moya, A. Dobermann, D. Dawe, Rice yields in tropical/subtropical Asia exhibit large but opposing sensitivities to minimum and maximum temperatures. *Proc. Natl. Acad. Sci. U.S.A.* **107**, 14562–14567 (2010).
15. Q. Su, J. S. Rohila, S. Ranganathan, R. Karthikeyan, Rice yield and quality in response to daytime and nighttime temperature increase – A meta-analysis perspective. *Sci. Total Environ.* **898**, 165256 (2023).
16. D. Xiong, X. Ling, J. Huang, S. Peng, Meta-analysis and dose-response analysis of high temperature effects on rice yield and quality. *Environ. Exp. Bot.* **141**, 1–9 (2017).
17. Y. Xu, C. Chu, S. Yao, The impact of high-temperature stress on rice: Challenges and solutions. *Crop J.* **9**, 963–976 (2021).
18. E. E. Rezaei, H. Webber, T. Gaiser, J. Naab, F. Ewert, Heat stress in cereals: Mechanisms and modelling. *Eur. J. Agron.* **64**, 98–113 (2015).
19. T. Sun, T. Hasegawa, B. Liu, L. Tang, L. Liu, W. Cao, Y. Zhu, Current rice models underestimate yield losses from short-term heat stresses. *Glob. Change Biol.* **27**, 402–416 (2021).
20. C. Müller, J. Jägermeyr, J. A. Franke, A. C. Ruane, J. Balkovic, P. Ciais, M. Dury, P. Falloon, C. Folberth, T. Hank, M. Hoffmann, R. C. Izaurralde, I. Jacquemin, N. Khabarov, W. F. Liu, S. Olin, T. A. M. Pugh, X. H. Wang, K. Williams, F. Zabel, J. W. Elliott, Substantial differences in crop yield sensitivities between models call for functionality-based model evaluation. *Earth's Futur.* **12**, e2023EF003773 (2024).
21. K. Kornhuber, C. Lesk, C. F. Schleussner, J. Jägermeyr, P. Pfleiderer, R. M. Horton, Risks of synchronized low yields are underestimated in climate and crop model projections. *Nat. Commun.* **14**, 3528 (2023).
22. R. S. Noia Junior, S. Asseng, C. Muller, J. C. Deswarte, J. P. Cohan, P. Martre, Negative impacts of climate change on crop yields are underestimated. *Trends Plant Sci.* **30**, 1262–1273 (2025).
23. K. van der Wiel, R. Bintanja, Contribution of climatic changes in mean and variability to monthly temperature and precipitation extremes. *Commun. Earth Environ.* **2**, 1 (2021).
24. C. J. Bernacchi, S. P. Long, D. R. Ort, Safeguarding crop photosynthesis in a rapidly warming world. *Science* **388**, 1153–1160 (2025).
25. J. A. Franke, C. Müller, J. Elliott, A. C. Ruane, J. Jägermeyr, J. Balkovic, P. Ciais, M. Dury, P. D. Falloon, C. Folberth, L. François, T. Hank, M. Hoffmann, R. C. Izaurralde, I. Jacquemin, C. Jones, N. Khabarov, M. Koch, M. Li, W. F. Liu, S. Olin, M. Phillips, T. A. M. Pugh, A. Reddy, X. H. Wang, K. Williams, F. Zabel, E. J. Moyer, The GGCMI phase 2 experiment: Global gridded crop model simulations under uniform changes in CO_2, temperature, water, and nitrogen levels (protocol version 1.0). *Geosci. Model Dev.* **13**, 2315–2336 (2020).
26. P. Zhu, Q. Zhuang, S. V. Archontoulis, C. Bernacchi, C. Müller, Dissecting the nonlinear response of maize yield to high temperature stress with model-data integration. *Glob. Chang. Biol.* **25**, 2470–2484 (2019).
27. L. Qiao, X. Wang, P. Smith, J. Fan, Y. Lu, B. Emmett, R. Li, S. Dorling, H. Chen, S. Liu, T. G. Benton, Y. Wang, Y. Ma, R. Jiang, F. Zhang, S. Piao, C. Müller, H. Yang, Y. Hao, W. Li, M. Fan, Soil quality both increases crop production and improves resilience to climate change. *Nat. Clim. Chang.* **12**, 574–580 (2022).
28. F. C. Moore, U. L. C. Baldos, T. Hertel, Economic impacts of climate change on agriculture: A comparison of process-based and statistical yield models. *Environ. Res. Lett.* **12**, 065008 (2017).
29. A. Hultgren, T. Carleton, M. Delgado, D. R. Gergel, M. Greenstone, T. Houser, S. Hsiang, A. Jina, R. E. Kopp, S. B. Malevich, K. E. McCusker, T. Mayer, I. Nath, J. Rising, A. Rode, J. Yuan, Impacts of climate change on global agriculture accounting for adaptation. *Nature* **642**, 644–652 (2025).
30. Q. Zhao, C. Wang, X. Wang, E. E. Rezaei, C. Müller, E. Wang, H. Webber, L. Zhang, X. Li, Y. Sang, G. Zhao, C. Folberth, A. Jain, W. Liu, M. Okada, F. Zabel, J. Jäegermeyr, H. Guo, Y. Zhang, Y. Jiang, F. Zhou, S. Piao, Temperature thresholds of extreme heat-induced yield loss in maize and soybean reveal geographic heterogeneity across the Northern Hemisphere. *Nat. Food* **7**, 194–205 (2026).
31. S. V. K. Jagadish, R. Muthurajan, Z. W. Rang, R. Malo, S. Heuer, J. Bennett, P. Q. Craufurd, Spikelet proteomic response to combined water deficit and heat stress in rice (*Oryza sativa* cv. N22). *Rice* **4**, 1–11 (2011).
32. W. Shi, X. Yin, P. C. Struik, C. Solis, F. Xie, R. C. Schmidt, M. Huang, Y. Zou, C. Ye, S. V. K. Jagadish, High day- and night-time temperatures affect grain growth dynamics in contrasting rice genotypes. *J. Exp. Bot.* **68**, 5233–5245 (2017).
33. J. Kim, J. Shon, C.-K. Lee, W. Yang, Y. Yoon, W.-H. Yang, Y.-G. Kim, B.-W. Lee, Relationship between grain filling duration and leaf senescence of temperate rice under high temperature. *Field Crop Res* **122**, 207–213 (2011).
34. F. Zhen, Y. Liu, I. Ali, B. Liu, L. Liu, W. Cao, L. Tang, Y. Zhu, Short-term heat stress at booting stage inhibited nitrogen remobilization to grain in rice. *J. Agric. Food Res.* **2**, 100066 (2020).
35. H. Yamakawa, T. Hirose, M. Kuroda, T. Yamaguchi, Comprehensive expression profiling of rice grain filling-related genes under high temperature using DNA microarray. *Plant Physiol.* **144**, 258–277 (2007).
36. C. Wu, S. Tang, G. Li, S. Wang, S. Fahad, Y. Ding, Roles of phytohormone changes in the grain yield of rice plants exposed to heat: A review. *PeerJ* **7**, e7792 (2019).

37. C. Lesk, W. Anderson, A. Rigden, O. Coast, J. Jägermeyr, S. McDermid, K. F. Davis, M. Konar, Compound heat and moisture extreme impacts on global crop yields under climate change. *Nat. Rev. Earth. Environ.* **3**, 872–889 (2022).
38. S. Siebert, H. Webber, G. Zhao, F. Ewert, Heat stress is overestimated in climate impact studies for irrigated agriculture. *Environ. Res. Lett.* **12**, 054023 (2017).
39. H. Webber, P. Martre, S. Asseng, B. Kimball, J. White, M. Ottman, G. W. Wall, G. De Sanctis, J. Doltra, R. Grant, B. Kassie, A. Maiorano, J. E. Olesen, D. Ripoche, E. E. Rezaei, M. A. Semenov, P. Stratonovitch, F. Ewert, Canopy temperature for simulation of heat stress in irrigated wheat in a semi-arid environment: A multi-model comparison. *Field Crop Res* **202**, 21–35 (2017).
40. H. Webber, J. W. White, B. A. Kimball, F. Ewert, S. Asseng, E. Eyshi Rezaei, P. J. Pinter, J. L. Hatfield, M. P. Reynolds, B. Ababaei, M. Bindi, J. Doltra, R. Ferrise, H. Kage, B. T. Kassie, K.-C. Kersebaum, A. Luig, J. E. Olesen, M. A. Semenov, P. Stratonovitch, A. M. Ratjen, R. L. LaMorte, S. W. Leavitt, D. J. Hunsaker, G. W. Wall, P. Martre, Physical robustness of canopy temperature models for crop heat stress simulation across environments and production conditions. *Field Crop Res* **216**, 75–88 (2018).
41. FAOSTAT, Crops and Livestock Products. www.fao.org/faostat.
42. B. Schauberger, S. Archontoulis, A. Arneth, J. Balkovic, P. Ciais, D. Deryng, J. Elliott, C. Folberth, N. Khabarov, C. Müller, T. A. M. Pugh, S. Rolinski, S. Schaphoff, E. Schmid, X. Wang, W. Schlenker, K. Frieler, Consistent negative response of US crops to high temperatures in observations and crop models. *Nat. Commun.* **8**, 13931 (2017).
43. A. M. Shew, J. B. Tack, L. L. Nalley, P. Chaminuka, Yield reduction under climate warming varies among wheat cultivars in South Africa. *Nat. Commun.* **11**, 4408 (2020).
44. D. Maraun, R. Schiemann, A. Ossó, M. Jury, Changes in event soil moisture-temperature coupling can intensify very extreme heat beyond expectations. *Nat. Commun.* **16**, 734 (2025).
45. Z. Zhou, L. Zhang, Q. Zhang, C. Hu, G. Wang, D. She, J. Chen, Global increase in future compound heat stress-heavy precipitation hazards and associated socio-ecosystem risks. *npj Clim. Atmos. Sci.* **7**, 33 (2024).
46. S. Heinicke, K. Frieler, J. Jägermeyr, M. Mengel, Global gridded crop models underestimate yield responses to droughts and heatwaves. *Environ. Res. Lett.* **17**, 044026 (2022).
47. J. Schewe, S. N. Gosling, C. Reyer, F. Zhao, P. Ciais, J. Elliott, L. Francois, V. Huber, H. K. Lotze, S. I. Seneviratne, M. T. H. van Vliet, R. Vautard, Y. Wada, L. Breuer, M. Buchner, D. A. Carozza, J. Chang, M. Coll, D. Deryng, A. de Wit, T. D. Eddy, C. Folberth, K. Frieler, A. D. Friend, D. Gerten, L. Gudmundsson, N. Hanasaki, A. Ito, N. Khabarov, H. Kim, P. Lawrence, C. Morfopoulos, C. Muller, H. Muller Schmied, R. Orth, S. Ostberg, Y. Pokhrel, T. A. M. Pugh, G. Sakurai, Y. Satoh, E. Schmid, T. Stacke, J. Steenbeek, J. Steinkamp, Q. Tang, H. Tian, D. P. Tittensor, J. Volkholz, X. Wang, L. Warszawski, State-of-the-art global models underestimate impacts from climate extremes. *Nat. Commun.* **10**, 1005 (2019).
48. L. L. Sloat, S. J. Davis, J. S. Gerber, F. C. Moore, D. K. Ray, P. C. West, N. D. Mueller, Climate adaptation by crop migration. *Nat. Commun.* **11**, 1243 (2020).
49. S. Minoli, J. Jägermeyr, S. Asseng, A. Urfels, C. Müller, Global crop yields can be lifted by timely adaptation of growing periods to climate change. *Nat. Commun.* **13**, 7079 (2022).
50. M. N. Li, S. W. Zhou, S. J. Shen, J. L. Wang, Y. H. Yang, Y. Z. Wu, F. Chen, Y. D. Lei, Climate-smart irrigation strategy can mitigate agricultural water consumption while ensuring food security under a changing climate. *Agric. Water Manag.* **292**, 108663 (2024).
51. Y. Bo, X. H. Wang, K. J. van Groenigen, B. A. Linquist, C. Müller, T. Li, J. C. Yang, J. Jägermeyr, Y. Qin, F. Zhou, Improved alternate wetting and drying irrigation increases global water productivity. *Nat. Food* **5**, 1005–1013 (2024).
52. D. B. Lobell, G. L. Hammer, G. McLean, C. Messina, M. J. Roberts, W. Schlenker, The critical role of extreme heat for maize production in the United States. *Nat. Clim. Change* **3**, 497–501 (2013).
53. W. Schlenker, M. J. Roberts, Nonlinear temperature effects indicate severe damages to U.S. crop yields under climate change. *Proc. Natl. Acad. Sci. U.S.A.* **106**, 15594–15598 (2009).
54. R. de S. Nóia Júnior, J. C. Deswarte, J. P. Cohan, P. Martre, M. van der Velde, R. Lecerf, H. Webber, F. Ewert, A. C. Ruane, G. A. Slafer, S. Asseng, The extreme 2016 wheat yield failure in France. *Glob. Chang. Biol.* **29**, 3130–3146 (2023).
55. A. C. Ruane, R. Goldberg, J. Chryssanthacopoulos, Climate forcing datasets for agricultural modeling: Merged products for gap-filling and historical climate series estimation. *Agric. For. Meteorol.* **200**, 233–248 (2015).
56. Q. Q. Kong, M. Huber, A global high-resolution and bias-corrected dataset of CMIP6 projected heat stress metrics. *Sci. Data* **12**, 246 (2025).
57. S. Supharatid, T. Aribarg, J. Nafung, Bias-corrected CMIP6 climate model projection over Southeast Asia. *Theor. Appl. Climatol.* **147**, 669–690 (2022).
58. FAO/IIASA/ISRIC/ISSCAS/JRC, Harmonized world soil database, version 1.2, FAO and IIASA (2012); https://www.fao.org/soils-portal/data-hub/soil-maps-and-databases/harmonized-world-soil-database-v12/en.
59. J. Koo, L. You, Z. Guo, U. Wood-Sichra, Y. Ru, S.-M. Jeon, Global spatially-disaggregated crop production statistics data for 2010, version 2.0 (2019); https://doi.org/10.7910/DVN/PRFF8V.
60. X. Deng, Y. Huang, W. Yuan, W. Zhang, P. Ciais, W. Dong, P. Smith, Z. Qin, Building soil to reduce climate change impacts on global crop yield. *Sci. Total Environ.* **903**, 166711 (2023).
61. J. Huang, A. E. Hartemink, C. J. Kucharik, Soil-dependent responses of US crop yields to climate variability and depth to groundwater. *Agr. Syst.* **190**, 103085 (2021).
62. F. J. P. Wankmüller, L. Delval, P. Lehmann, M. J. Baur, A. Cecere, S. Wolf, D. Or, M. Javaux, A. Carminati, Global influence of soil texture on ecosystem water limitation. *Nature* **635**, 631–638 (2024).
63. C. Ye, G. J. Zheng, Y. Tao, Y. N. Xu, G. Chu, C. M. Xu, S. Chen, Y. H. Liu, X. F. Zhang, D. Y. Wang, Effect of soil texture on soil nutrient status and rice nutrient absorption in paddy soils. *Agronomy* **14**, 1339 (2024).
64. P. R. Steward, A. J. Dougill, C. Thierfelder, C. M. Pittelkow, L. C. Stringer, M. Kudzala, G. E. Shackelford, The adaptive capacity of maize-based conservation agriculture systems to climate stress in tropical and subtropical environments: A meta-regression of yields. *Agric. Ecosyst. Environ.* **251**, 194–202 (2018).
65. A. Williams, M. C. Hunter, M. Kammerer, D. A. Kane, N. R. Jordan, D. A. Mortensen, R. G. Smith, S. Snapp, A. S. Davis, Soil water holding capacity mitigates downside risk and volatility in US rainfed maize: Time to invest in soil organic matter? *PLOS ONE* **11**, e0160974 (2016).
66. E. E. Rezaei, S. Siebert, R. Manderscheid, J. Müller, A. Mahrookashani, B. Ehrenpfordt, J. Haensch, H. J. Weigel, F. Ewert, Quantifying the response of wheat yields to heat stress: The role of the experimental setup. *Field Crop Res* **217**, 93–103 (2018).

Acknowledgments: We acknowledge the crop modeling groups for producing and making available their model outputs. We thank K. Cui and D. Xiong from Huazhong Agricultural University and Y. Xu from Henan Agricultural University for guidance on mechanisms explaining the impact of high temperature on rice growth. We also thank T. Hasegawa for comments that helped improve the manuscript. **Funding:** This work was supported by National Natural Science Foundation of China [42225102 (F.Z.), 42361144876 (F.Z.), and 32172129 (Z.S.)] as well as Scientific Research Innovation Capability Support Project for Young Faculty [ZYGXQNJSKYCXNLZCXM-S2 (X.W.)]. **Author contributions:** Conceptualization: F.Z., X.W., Y.J., P.C., and P.Z. Methodology: Y.J., X.W., F.Z., J.J., and P.C. Resources: F.Z., J.J., C.M., K.C., and S.H. Data curation: Y.J., C.M., J.J., and J.H. Validation: Y.J. and J.H. Formal analysis: Y.J., F.Z., and B.W. Investigation: Y.J., F.Z., B.W., J.H., Z.Z., and Y.J. Visualization: Y.J. and J.J. Supervision: F.Z., X.W., and Y.J. Project administration: Y.J. and F.Z. Funding acquisition: F.Z. and Z.S. Writing—original draft: Y.J., F.Z., X.W., P.C., and P.Z. Writing—review and editing: Y.J., X.W., P.C., C.M., J.Z., J.J., T.L., P.Z., K.C., P.H., S.H., Y.J., Z.S., and Z.Z. **Competing interests:** The authors declare that they have no competing interests. **Data, code, and materials availability:** All data and code needed to evaluate and reproduce the results in the paper are present in the paper and/or the Supplementary Materials. The field-warming experiments dataset used in this study is available at data S1. Gridded crop model outputs from GGCMI phase 2 experiments are available through Zenodo for each crop model used in this study: CARAIB (https://zenodo.org/records/2582504), EPIC-TAMU (https://zenodo.org/records/2582352), GEPIC (https://zenodo.org/records/2582251), LPJmL (https://zenodo.org/records/4384615), pDSSAT (https://zenodo.org/records/2582127), PEPIC (https://zenodo.org/records/2582343), and PROMET (https://zenodo.org/records/2582479). Additional details are provided in Franke *et al.* (*25*). AgMERRA climate dataset is available at https://data.giss.nasa.gov/impacts/agmipcf/agmerra/. Climate projections from CMIP6 are available at https://data.isimip.org/search/tree/ISIMIP3b/InputData/climate/atmosphere/. All analysis codes have been deposited in Zenodo and are available at https://doi.org/10.5281/zenodo.17314177. This study did not generate new materials.

Submitted 15 November 2025
Accepted 26 June 2026
Published 29 July 2026
10.1126/sciadv.aed9226

Science Advances

Vulnerability to high temperature shapes global warming impacts on rice yield

Yiwei Jian, Xuhui Wang, Jonas Jägermeyr, Philippe Ciais, Christoph Müller, Jakob Zscheischler, Tao Li, Kun Cheng, Pengfu Hou, Jianliang Huang, Shan Huang, Yu Jiang, Bin Wang, Zhenwei Song, Zuolin Zhang, Peng Zhu, and Feng Zhou

Sci. Adv. **12** (31), eaed9226. DOI: 10.1126/sciadv.aed9226

View the article online
https://www.science.org/doi/10.1126/sciadv.aed9226
Permissions
https://www.science.org/help/reprints-and-permissions

Science Advances (ISSN 2375-2548) is published by the American Association for the Advancement of Science. 1200 New York Avenue NW, Washington, DC 20005. The title *Science Advances* is a registered trademark of AAAS.